J|A|C|S
ARTICLES
Published on Web 12/24/2002

Antibody Recognition of Chiral Surfaces. Enantiomorphous Crystals of Leucine-Leucine-Tyrosine

Merav Geva,[†] Felix Frolow,[‡,§] Miriam Eisenstein,[‡] and Lia Addadi*[,†]

Contribution from the Departments of Structural Biology and Chemical Services, Weizmann Institute of Science, 76100 Rehovot, Israel

Received July 31, 2002; E-mail: lia.addadi@weizmann.ac.il

Abstract: Monoclonal antibodies were selected after immunization with crystals of the tripeptide L-leucine-L-leucine-L-tyrosine. They interact with the tripeptide crystals, but do not interact with the tripeptide molecule, with other crystalline surfaces, or with adsorbed protein. The interactions of two antibodies with crystals of L-Leu-L-Leu-L-Tyr and of its enantiomer D-Leu-D-Leu-D-Tyr were characterized in depth. Antibody 48E is stereoselective and enantioselective: it recognizes only the $\{0\bar{1}1\}$ faces of the L-Leu-L-Leu-L-Tyr crystals, and not the enantiomorphous $\{01\bar{1}\}$ faces of D-Leu-D-Leu-D-Tyr crystals, or any other faces of either crystal. In contrast, antibody 602E is poorly stereoselective and is not enantioselective: it recognizes the crystals of both enantiomers, interacting with a number of different faces of each. The different recognition patterns are explained on the basis of the nature of the interactions and the structure of the interacting surfaces. Understanding this antibody specificity advances our general understanding of surface recognition and transfer of chiral information across biological interfaces.

Introduction

The intimate association between life and chirality is amply manifested in biological processes. While chirality is well understood at the molecular level, however, a lot is still missing in the transition from molecular chirality to the dissimmetry expressed at the higher length scales of surfaces and materials. This is often at the basis of recognition and plays an important role in the development of asymmetry in biology. We wish to understand how chiral information can be transferred from molecules to material surfaces, or vice versa, in other words how stereochemistry influences biology from the length scale of nanometers to micrometers and millimeters, many orders of magnitude larger than the length scale of molecules.

Transfer of chiral information from biological molecules to material surfaces is observed in a number of biomineralization processes, which involve crystal growth in the presence of biological macromolecules. Biological macromolecules induce morphologies of invariant chirality in crystals which do not have an inherently chiral structure. Such reduction in symmetry was observed in single biogenic crystals, such as sponge spicules,[2] coccoliths,[3] magnetite crystals from magnetotactic bacteria,[4] and calcium oxalate crystals from plant leaves.[5] Interestingly, ice interacts enantioselectively with antifreeze polypeptides.[6,7] The same concepts were applied in vitro in the induction of chiral morphology by amino acids[8] and porphyrin monolayers[9] in calcite. Likewise, amino acid monolayers and other chiral additives were shown to display chiral recognition on crystals of achiral glycine[10,11] or racemic compounds.[12,13] In the latter examples, it was possible to explain the molecular mechanism of chiral recognition in detail. In the examples taken from biology, however, this is extremely difficult, if at all possible.

We have thus undertaken a project to study chiral recognition on surfaces in biological systems, using crystals as substrates and antibodies as the recognition tool. A previous study of the interactions of antibodies with crystals and monolayers showed an impressive degree of complementarity between specific antibodies and the organized surfaces that served as antigens.[14,15]

[†] Department of Structural Biology.
[‡] Department of Chemical Services.
[§] Present address: Department of Molecular Microbiology and Biotechnology, Tel Aviv University, Tel Aviv 69978, Israel.

(1) We chose to use here the notation commonly used for amino acids, namely, L and D. We note that the correct notation, following Cahn Ingold and Prelog rules, is (*S*)-leucine-(*S*)-leucine-(*S*)-tyrosine for the L-enantiomer and (*R*)-leucine-(*R*)-leucine-(*R*)-tyrosine for the D-enantiomer.
(2) Aizenberg, J.; Hanson, J.; Koetzle, T.; Leiserowitz, L.; Weiner, S.; Addadi, L. *Chem.—Eur. J.* **1995**, *1*, 414−422.
(3) Young, J. R.; Davis, S. A.; Bown, P. R.; Mann, S. *J. Struct. Biol.* **1999**, *126*, 195−215.
(4) Mann, S.; Sparks, N. H. C.; Blakemore, R. P. *Proc. R. Soc. London, B* **1987**, *231*, 477−487.
(5) Bouropoulos, N.; Weiner, S.; Addadi, L. *Chem.—Eur. J.* **2001**, *7*, 1881−1888.
(6) Laursen, R. A.; Wen, D. Y.; Knight, C. A. *J. Am. Chem. Soc.* **1994**, *116*, 12057−12058.
(7) Wierzbicki, A.; Taylor, M. S.; Knight, C. A.; Madura, J. D.; Harrington, J. P.; Sikes, C. S. *Biophys. J.* **1996**, *71*, 8−18.
(8) Orme, C. A.; Noy, A.; Wierzbicki, A.; McBride, M. T.; Grantham, M. T., H. H.; Dove, P. M.; DeYoreo, J. J. *Nature* **2001**, *411*, 775−779.
(9) Lahiri, L.; Xu, G.; Dabbs, D. M.; Yao, N.; Aksay, I. A.; Groves, J. T. *J. Am. Chem. Soc.* **1997**, *119*, 5449−5450.
(10) Landau, E. M.; Levanon, M.; Leiserowitz, L.; Lahav, M.; Sagiv, J. *Nature* **1985**, *318*, 353−356.
(11) Weissbuch, I.; Addadi, L.; Lahav, M.; Leizerowitz, L. *Science* **1991**, *253*, 637−645.
(12) Addadi, L.; Berkovitch-Yellin, Z.; Weissbuch, I.; Lahav, M.; Leiserowitz, L.; Weinstein, S. *J. Am. Chem. Soc.* **1982**, *104*, 2075.
(13) Lahav, M.; Leiserowitz, L. *Angew. Chem., Intl. Ed.* **1999**, *38*, 2533−2536.
(14) Bromberg, R.; Kessler, N.; Addadi, L. *J Cryst. Growth* **1998**, *193*, 656−664.
(15) Kessler, N.; Perl-Treves, D.; Addadi, L.; Eisenstein, M. *Proteins: Struct., Funct., Genet.* **1999**, *34*, 383−394.

10.1021/ja027942j CCC: $25.00

By definition, enantiomeric surfaces form diastereomeric complexes with a specific antibody, and thus should be different vis-à-vis the antibody. Such examples at the molecular length scale are abundant in biology and in antibody−antigen interactions as well.[16−18] The extent of chiral recognition at crystal surfaces however depends heavily on the dissimmetry expressed on the chiral surface,[19,20] as well as on the resolution of the interactions between the antibody and the surface. We have recently raised and selected one antibody against crystals of cholesterol monohydrate, which has very high affinity also for monolayers of cholesterol at the air−water interface.[21,22] This antibody was shown to be highly stereoselective, but not enantioselective, inasmuch as it recognized cholesterol and *ent*-cholesterol (but not epicholesterol) monolayers with the same high affinity.[23] The absence of enantioselectivity was attributed to the low level of dissimmetry expressed on the interacting surface. Notwithstanding the fact that the surface is, by definition, chiral, the close packing of the molecules prevents molecular recognition of the hand-in-glove type. A surface-to-surface recognition rather applies, which does not appear to be influenced, in the case of cholesterol, by molecular chirality.

Here, we have studied molecular recognition of antibodies on surfaces of crystals of the tripeptide L-leucine-L-leucine-L-tyrosine.[1,24] Enantiomorphism was used as a tool to test recognition. Antibodies were selected against crystals of the LLL-enantiomer, and their recognition was then characterized on both enantiomeric crystals, LLL and DDD. The use of peptide crystals introduces antigenic surfaces that may resemble, to some extent, protein surfaces, nevertheless preserving the advantages of a repetitive lattice whose structure is known at the atomic level. A tripeptide is too short to be processed by the immune system through the "classical pathway"[25] by which proteins and polypeptides are processed. It is thus guaranteed that antibodies will not be elicited against the single molecules, but rather against arrays of molecular moieties exposed on the crystal surface.

Two antibodies were shown to interact with the chiral surfaces at different levels of stereo- and enantioselectivity, implying that they "feel" the same surface at a different resolution. One antibody is stereoselective and enantioselective, while the other has low stereoselectivity and no enantioselectivity. Understanding this antibody specificity advances our understanding of surface recognition in biological systems.

Experimental Section

Materials and Equipment. Amino acids and protected amino acids were purchased from Bachem Ag (Switzerland). Solvents and reagents were purchased from Sigma-Aldrich Israel Ltd. (Rehovot, Israel). ImmunoPure IgM purification kit no. 44897 was purchased from Pierce (Rockford, IL). Secondary antibodies for enzyme-linked immunosorbent assay (ELISA) were purchased from Jackson ImmunoResearch Inc. (West-Grove, PA). The Vector-Red alkaline phosphatase substrate kit was purchased from Vector Laboratories Inc. (Burlingame, CA). Color-labeled crystals were viewed and photographed with a Nikon (Japan) microscope equipped with a Lumina 2.2 CCD camera.

Synthesis of L-Leucine-L-Leucine-L-Tyrosine and D-Leucine-D-Leucine-D-Tyrosine. *N-t*-Boc-Leu (6.7 g) and *N*-hydroxysuccinimide (4.0 g) were dissolved in an ethyl acetate (100 mL)/dimethylformamide (5 mL) mixture and cooled to 0 °C in an ice−water bath. Dicyclohexylcarbodiimide (6.5 g), dissolved in ethyl acetate (30 mL), was added. The reaction mixture was stirred for 1 h in an ice−water bath and left overnight at room temperature. The dicyclohexylurea formed was filtered, and the ethyl acetate was evaporated from the filtrate. The activated *N-t*-Boc-Leu-succinimide was dissolved in dioxane (150 mL), and a solution of leucine (4.0 g) in 0.6 M $NaHCO_3$ (150 mL) was gradually mixed with the activated *N-t*-Boc-Leu-succinimide solution. The reaction mixture was stirred overnight at room temperature and then concentrated under vacuum. Water (100 mL) was added to the original solution, which was then acidified with concentrated HCl to pH 2. After 30 min in ice, the product *N-t*-Boc-Leu-Leu was filtered and dried under vacuum. *N-t*-Boc-Leu-Leu was activated in a procedure similar to the *N-t*-Boc-Leu activation, and dissolved in dioxane. Tyr-(*t*-Bu) (3.5 g) was dissolved in a 0.6 M $NaHCO_3$ (100 mL)/dioxane (100 mL) mixture, and gradually mixed with the activated *N-t*-Boc-Leu-Leu in dioxane solution. The reaction mixture was stirred overnight at room temperature, and then concentrated under vacuum. The product *N-t*-Boc-Leu-Leu-Tyr(*t*-Bu) was isolated by acidification as described for *N-t*-Boc-Leu-Leu. The protecting groups were removed simultaneously by 2 h incubation in a mixture of 90% H_2O, 5% trifluoroacetic acid, and 5% triethylsilane (total 100 mL). The solvents were evaporated, and the residue was triturated with ether (500 mL) and dried under vacuum. Leu-Leu-Tyr was cleaned on a silica column, eluted by a gradient of chloroform/methanol, 9:1 to 6:4. The final yield was 5 g of Leu-Leu-Tyr (40 mol %). The whole procedure was monitored by TLC in chloroform/methanol, 9:1, stained by potassium permanganate. A commercial sample of L-leucine-L-leucine-L-tyrosine was used as a reference. The product was identified by X-ray crystallography, circular dichroism (CD), and NMR. The CD spectra gave $[\theta]_{225} = +26000$ (deg cm^2)/dmol and $[\theta]_{210} = +20000$ (deg cm^2)/dmol and $[\theta]_{225} = -26000$ (deg cm^2)/dmol and $[\theta]_{210} = -20000$ (deg cm^2)/dmol for L-leucine-L-leucine-L-tyrosine and D-leucine-D-leucine-D-tyrosine, respectively. ^{1}H NMR spectrum in CD_3OH (Bruker 400 MHz): δ 0.83−0.89 (CH_3 of leucines 1 and 2, 12H); 1.47−1.52 (CH, CH_2 of leucines 1 and 2, 6H); 2.8−3.1 (CH_2 of tyrosine, 2H); 3.6 (CHα of leucine1, 1H); 4.3−4.4 (CHα of leucine 2 and tyrosine, 2H); 6.8, 7.1 (aromatic H atoms of tyrosine, 4H).

Crystallization of Leucine-Leucine-Tyrosine. Crystals of L-Leu-L-Leu-L-Tyr for X-ray analysis were grown using the hanging drop method from a 10 μL drop of a mixture of 80% water/20% 2-propanol and a reservoir of 1 mL of a mixture of 90% water/10% 2-propanol. The crystals grew within 48 h, at room temperature. Crystals of L-Leu-L-Leu-L-Tyr for immunizations were grown in glass test tubes, from mixtures of 70% water/30% 2-propanol, at room temperature. After 24 h, the mother liquor was removed and the crystals were suspended (4 mg/mL) in phosphate buffered saline (PBS) saturated with Leu-Leu-Tyr. Crystals of L-Leu-L-Leu-L-Tyr and D-Leu-D-Leu-D-Tyr for ELISA were grown in bovine serum albumin (BSA)-coated polystyrene 24-well tissue culture dishes (Nunclon). The peptide was dissolved in a mixture of 70% water/30% 2-propanol by heating (10 g/L). Upon boiling the solution was removed from the hot plate and allowed to cool for 5 min. Aliquots of 0.4 mL were placed in each well and seeded by adding minute amounts of crushed crystals. The plate was covered and left at room temperature for 48 h. The crystals grew, adhering to the bottom of the well. The supernatant was then removed, and the

(16) Guichard, G.; Benkirane, N.; Zeder-Lutz, G.; Van-Regenmortel, M. H. V.; Briand, J. P.; Muller, S. *Proc. Natl. Acad. Sci. U.S.A.* **1994**, *91*, 9765−9769.
(17) Hofstetter, O.; Hofstetter, H.; Schurig, V.; Wilchek, M.; Green, B. S. *J. Am. Chem. Soc.* **1998**, *120*, 3251−3252.
(18) Lee, S. B.; Mitchell, D. T.; Trofin, L.; Nevanen, T. K.; Soderlund, H.; Martin, C. R. *Science* **2002**, *292*, 2198−2200.
(19) Mislow, K.; Bickart, P. *Isr. J. Chem.* **1977**, *15*, 1−6.
(20) Zabrodsky, H.; Avnir, D. *J. Am. Chem. Soc.* **1995**, *117*, 462−473.
(21) Perl-Treves, D.; Kessler, N.; Izhaky, D.; Addadi, L. *Chem. Biol.* **1996**, *3*, 567−577.
(22) Izhaky, D.; Addadi, L. *Adv. Mater.* **1998**, *10*, 1009−1013.
(23) Geva, M.; Izhaky, D.; Mickus, D. E.; Rychnovsky, S. D.; Addadi, L. *ChemBioChem* **2001**, *2*, 265−271.
(24) Berthou, J.; Migliore-Samour, D.; Lifchitz, A.; Delletre, J.; Floch, F.; Jolles, P. *FEBS Lett.* **1987**, *218*, 55−58.
(25) Abbas, A. K. *Cellular and Molecular Immunology*, 2nd ed.; W. B. Saunders Co.: Philadelphia, 1994.

crystals were washed with water and kept in a desiccator under a humid atmosphere to avoid loss of lattice water. Plates were coated with BSA by 1 h incubation of the plates with 0.5 mL/well of 1% BSA in PBS, followed by three 30 min incubations with PBS.

Crystal Structure Determination. The crystals were measured on an AFC5R diffractometer using Mo radiation, $\lambda = 0.71069$ Å, 1.2° ω scans, speed 8 deg/min. Data were collected between $2\theta = 4°$ and $2\theta = 55°$, and processed using the XTAL3.2 package. The structure was solved by direct methods using SHELXS97, and refined by full-matrix least squares against F^2 using SHELXL97. Initial crystal morphology was established on the diffractometer, by establishing which plane was in the diffraction position when each face was viewed edge on. Routine assignment of crystal faces was done by measuring the dihedral angles between the faces, relative to the (001) plate face, in the scanning electron microscope. The crystal structure of L-Leu-L-Leu-L-Tyr was deposited in the Cambridge Structural Database (reference code CCDC181810).

Antibody Production. Crystal suspensions of 4 mg/mL L-Leu-L-Leu-L-Tyr in PBS saturated with L-Leu-L-Leu-L-Tyr were used to immunize six balb/c female mice, 10 weeks old when the immunizations were started. Three mice were immunized by surgically implanting crystals in the spleen twice at three weeks intervals, followed by three subcutaneous injections at three week intervals. Three additional mice were immunized by five subcutaneous injections at three week intervals. Two mice were immunized interperitoneally one week before the fusion, one of which was initially immunized in the spleen and the other one subcutaneously only. All animals were bled a week after every other immunization, and the serum containing polyclonal antibody population was tested on L-Leu-L-Leu-L-Tyr crystals by ELISA. Hybridoma selection was done by ELISA as described below.

Enzyme-Linked Immunosorbent Assay. Leu-Leu-Tyr crystals, grown in a 24-well multidish precoated with BSA, were first incubated with the hybridoma solution. The tested antibody or serum was diluted 1:100 to 1:1000 in binding buffer (0.5% (w/v) BSA in PBS, saturated overnight with Leu-Leu-Tyr and filtered), and 0.2 mL aliquots were applied to each well and incubated for 1 h. The unbound antibody was removed by washing three times with washing buffer (PBS saturated overnight with Leu-Leu-Tyr, filtered). The secondary antibody, alkaline phosphatase conjugated goat antimouse $F(ab)_2$, was diluted 1:1000 in binding buffer. Aliquots of 0.2 mL/well were incubated for 1 h, and then washed three times with washing buffer. For the standard color reaction, *p*-nitrophenyl phosphate was dissolved (1 mg/mL) in substrate buffer (10% triethanolamine buffer (pH 9.8) containing 0.01% $MgCl_2$ and 0.02% NaN_3) and 0.2 mL/well aliquots were incubated for 30 min. The color reaction was stopped by 50 μL/well 0.1 M EDTA. For detection, 0.2 mL from each well was transferred to a 96-well tissue culture dish, and absorbance was measured at 405 nm. For the in situ color reaction, Vector-Red substrate was used according to the manufacturer's instructions. Antibodies for these immunolabeling procedures were purified from ascites fluid by affinity chromatography using an ImmunoPure IgM purification column, according to the manufacturer's instructions. The purified antibody was extensively dialyzed against PBS, and stored at 4 °C.

Results

The tripeptide L-Leu-L-Leu-L-Tyr is an immunostimulant present in breast-milk casein.[24] Its crystals were chosen as an appropriate antigen both because of its activity in vivo and because of its low solubility in physiological fluids. L-Leu-L-Leu-L-Tyr and D-Leu-D-Leu-D-Tyr were synthesized from the corresponding L- and D-amino acids using classical peptide synthesis techniques.[26] The synthesis and purification procedures were exactly the same for the two enantiomers, and so was the enantiomeric purity (>99%) of the final products.

Crystal Packing and Morphology. L-Leu-L-Leu-L-Tyr crystallizes from water as a monohydrate, in space group $P2_1$, $a = 5.7650(10)$ Å, $b = 17.053(3)$ Å, $c = 11.470(2)$ Å, $\beta = 99.09°$, and $Z = 2$.

The tripeptide molecules pack in a highly polar structure, such that the peptide backbone is by and large parallel to the polar *b* axis (Figure 1). The N-terminals all point toward $+b$, while the C-terminal carboxylates and the aromatic rings of the tyrosine residues all point toward $-b$. The polar packing is reflected in the crystals growing in a polar morphology. While the L-Leu-L-Leu-L-Tyr crystals grow in a variety of morphologies, ranging from trapezoidal and triangular prisms to almost semicircular wedges depending upon the specific conditions, they always develop as asymmetrically shaped {001} plates (Figure 2). In particular, the negative direction of the polar *b* axis is always delimited by the $\{0\bar{1}1\}$ faces (namely, $(0\bar{1}1)$ and $(0\bar{1}\bar{1})$), while the positive direction of the polar *b* axis is delimited by various faces of the {0*kl*} family. In the ⟨100⟩ direction, the crystals are limited by faces of the {*hk*0} family. Stacking interactions between tyrosine rings are mainly responsible for the relatively large rate of growth of the crystal in this direction, while hydrogen-bonding and ionic interactions link together uninterrupted molecular chains along *b*. Mainly hydrophobic interactions, with the exception of H-bonds between tyrosine hydroxyls and peptide carbonyls, define the structure along *c*. This is probably the reason the crystals grow as {001} plates. {001} faces are characterized by an undulating surface where the leucine side chains, the carboxylate terminus, and the hydroxyl group on the aromatic ring of tyrosine emerge to some extent. The $\{0\bar{1}1\}$ faces may form as rather flat surfaces exposing carboxylates and tyrosine rings of tripeptide molecules 1 and 2, respectively (as defined in Figure 1), besides the hydrophobic side chains of leucines. We note that molecule 2 exposes on this face an essentially hydrophobic surface. In water, it might be thus expected that, at equilibrium, molecule 2 will be removed from the surface, resulting in an undulating surface (highlighted in Figure 1a) including grooves with exposed ammonium and carboxylate groups in addition to tyrosine hydroxyls, while the ridges would expose the carboxylate group and the side chains of one leucine, all molecules of type 1. This would result in a much more hydrophilic surface, with a more favorable surface interaction energy with water.

In contrast to the $-b$ direction, the {011} faces that delimit the crystals in the $+b$ direction expose, besides hydrophobic side chains, the ammonium group of the amino terminal. The lateral {*hk*0) faces are rather flat and densely packed, with few available hydrogen-bonding interactions exposed.

Crystals of D-Leu-D-Leu-D-Tyr have by definition the same packing interactions and the same structure as L-Leu-L-Leu-L-Tyr, apart from the molecules having opposite absolute configuration and being oriented opposite relative to the polar *b* axis.[27] The crystal morphology will consequently also be opposite, the base of the triangle being delimited by the $\{01\bar{1}\}$ faces (namely, $(01\bar{1})$ and (011)) in the crystal of D-Leu-D-Leu-D-Tyr (Figure 2).

(26) Fridkin, M.; Hazum, E.; Tauber-Finkelstein, M.; Shaltiel, S. *Arch. Biochem. Biophys.* **1977**, *178*, 517−526.

(27) Addadi, L.; Berkovitch-Yellin, Z.; Weissbuch, I.; Lahav, M.; Leiserowitz, L. In *Topics in Stereochemistry*; Eliel, E. L., Wilen, S. H., Allinger, N. H., Eds.; John Wiley & Sons: New York, 1986, Vol. 16.

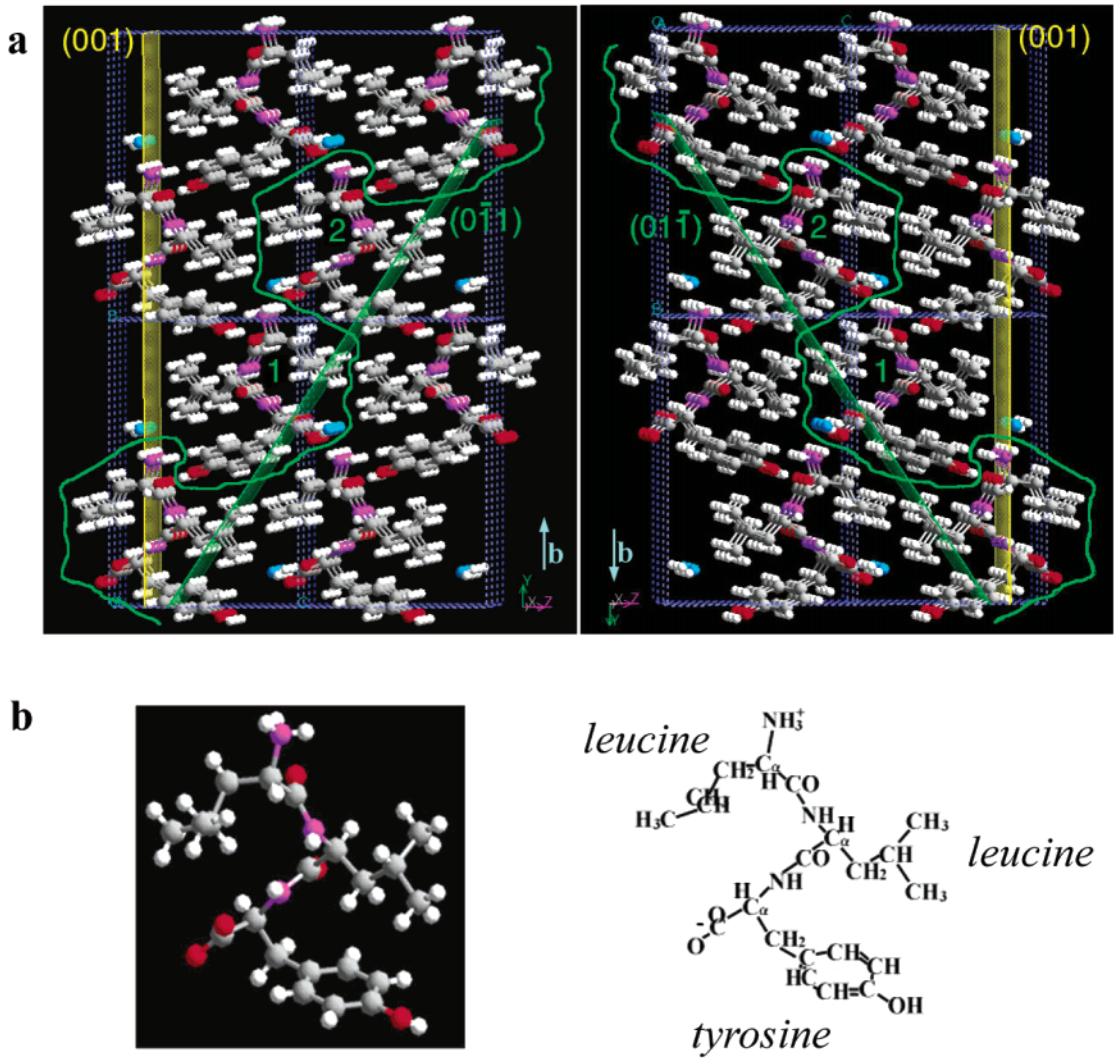

Figure 1. (a) Packing diagram of L-Leu-L-Leu-L-Tyr (left) and D-Leu-D-Leu-D-Tyr (right), viewed almost parallel to the *bc* plane. Three unit cells are shown in the perpendicular direction to show the stacking interactions between the molecules in that direction. The (001) plane is shown in yellow. The (0$\bar{1}$1) and (01$\bar{1}$) planes (for the L,L,L and D,D,D crystals, respectively) are shown in green. The undulating surface that is obtained by removing molecules of type 2 from the surface is represented by the green trace. Note that the positive direction of the *b* axis points upward in the left picture, and downward in the right picture. Atom color code: carbon, gray; hydrogen, white; oxygen, red; nitrogen, magenta; water oxygen, cyan. (b) Structure (left) and formula (right) of L-Leu-L-Leu-L-Tyr molecule 2, taken from the packing diagram in the same orientation, to facilitate identification.

The extent to which the different crystal faces express chirality is difficult to evaluate. Clearly all faces are chiral by definition, independent of whether chiral carbons are directly exposed on it. The close packing of the molecules, however, may be expected to interfere with molecular chiral recognition.

Characterization of Antibody Specificity. Antibodies were produced by immunizing mice against crystals of L-Leu-L-Leu-L-Tyr, followed by conventional fusion and selection.[21,28−30] As the peptides have relatively low solubility in water (0.67 g/L), the crystals do not readily dissolve in physiological buffers.

The antibodies were screened against three sets of substrates: L-Leu-L-Leu-L-Tyr crystals, BSA-coated polystyrene surfaces, and 1,4-dinitrobenzene (DNB) crystals. The BSA-coated polystyrene control was used to eliminate antibodies that bind adsorbed proteins, whereas the DNB crystals were used to detect antibodies that bind to any crystalline surfaces.

Screening of the antibodies was performed by ELISA, on the basis of which antibodies were characterized as nonreactive (to L-Leu-L-Leu-L-Tyr crystals), nonspecific (i.e., binding to both DNB and L-Leu-L-Leu-L-Tyr crystals), or specific (binding to L-Leu-L-Leu-L-Tyr crystals, but not reactive to adsorbed BSA or DNB crystals). Two antibodies, 48E and 602E, which belong to the last (specific) group, were selected for further study.

Following the first screening, the selected antibody binding and specificity were checked on crystals of L-Leu-L-Leu-L-Tyr and D-Leu-D-Leu-D-Tyr. All external surfaces, excluding those of the crystals, used for antibody binding analysis were precoated with BSA to avoid nonspecific adsorption of the antibodies to the surface. Tissue culture dishes where crystals of L-Leu-L-Leu-L-Tyr and D-Leu-D-Leu-D-Tyr were grown directly attached to the dish surface were incubated in parallel with antibody in the presence of excess BSA, and their binding patterns were analyzed by in situ color development ELISA with the Vector-Red substrate kit.[14] Using this technique, the developed color is confined to the specific location where the

(28) Kessler, N.; Perl-Treves, D.; Addadi, L. *FASEB J.* **1996**, *10*, 1435−1442.
(29) Kohler, G.; Milstein, C. *Nature* **1974**, *256*, 495−497.
(30) Eshhar, Z. In *Monoclonal antibody strategy and techniques*; Springer, T. A., Ed.; Plenum Press: New York, 1985; pp 3−41.

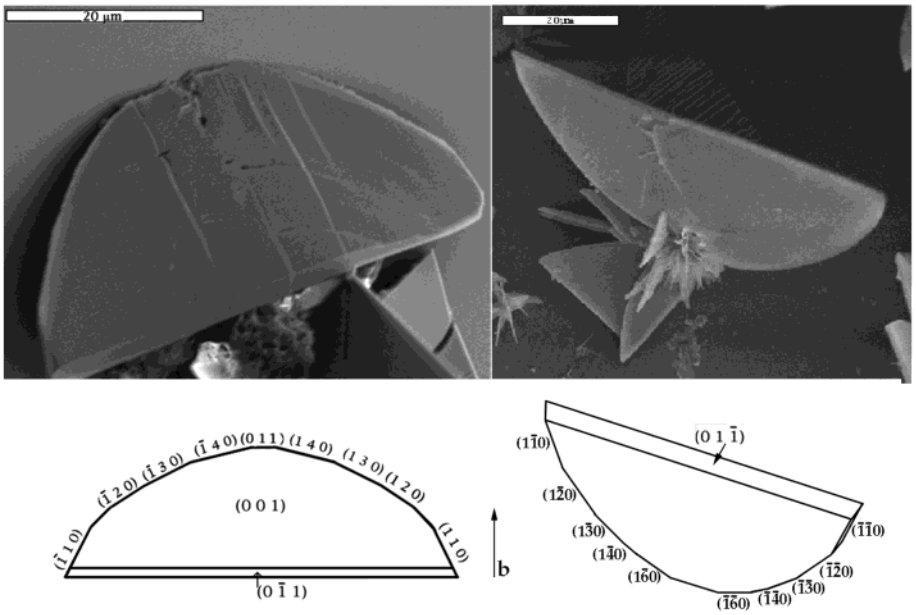

Figure 2. Scanning electron micrographs (top) and derived morphologies (bottom) of representative crystals of L-Leu-L-Leu-L-Tyr (left) and D-Leu-D-Leu-D-Tyr (right). Note that the direction of the *b* axis is the same for both crystals.

antibodies are bound. This enables us to detect binding and crystal face specificity.

(1) Antibody 48E. Crystals of L-Leu-L-Leu-L-Tyr incubated with antibody 48E developed red color exclusively on the {0$\bar{1}$1} faces. In contrast, crystals of D-Leu-D-Leu-D-Tyr incubated with this antibody did not develop color on any crystal face (Figure 3). The experiments were performed in parallel with the two enantiomers during the same day, using the same solutions. Five sets of experiments, each involving hundreds of crystals, were performed. Although the color develops on a relatively small area, its detection is straightforward on the white-green background of the other crystal faces. We evaluate that, in each experiment, approximately 95% of the crystals gave positive reaction on the L-Leu-L-Leu-L-Tyr crystals, while >95% of D-Leu-D-Leu-D-Tyr crystals gave negative reaction. We thus conclude that antibody 48E binds stereospecifically and enantiospecifically to the {0$\bar{1}$1} faces of the L-Leu-L-Leu-L-Tyr crystals.

(2) Antibody 602E. Crystals of L-Leu-L-Leu-L-Tyr incubated with antibody 602E developed red color on the {0$\bar{1}$1} faces, as well as on all circumferential {*hk*0} faces. No color was observed on the {001} plate faces. Crystals of D-Leu-D-Leu-D-Tyr incubated with this antibody exhibited the same color development on the {0$\bar{1}$1} faces and the {*hk*0} faces (Figure 4). Antibody 602E thus binds to the {0$\bar{1}$1} faces and to the surrounding {*hk*0} faces of both the L-Leu-L-Leu-L-Tyr and D-Leu-D-Leu-D-Tyr crystals, showing low specificity. The lower specificity of this antibody is expressed by its binding to several different crystal faces as well as by the lack of chiral discrimination of the antibody, despite the chirality expressed at the crystal faces to which it binds.

The keys to understanding the chiral discrimination are in the comparison between the structures of the {0$\bar{1}$1} faces in the L-Leu-L-Leu-L-Tyr relative to the D-Leu-D-Leu-D-Tyr crystal, as well as between the structures of the {0$\bar{1}$1} faces and other faces, such as {001}, which are not recognized by either antibody. In addition, analysis of the antibody variable region se sequences and geometries relative to each other and to the bound surfaces will assist in understanding the factors responsible for the differential recognition (or lack thereof) of the two antibodies.

The (0$\bar{1}$1) structure depicted in Figure 5 refers to the ridge and groove model discussed in the analysis of the crystal packing (Figure 1). On the crystal surface, however, the molecules are in dynamic equilibrium with molecules in the solution, constantly attaching and detaching from the surface. The local structure of each crystal face may thus be represented by a combination of different molecular entities, all pertaining to the same face, provided that their structural and geometrical determinants are preserved. Thus, on the {0$\bar{1}$1} faces, the ridge and groove motif may not be present all of the time over all of the area.

Figure 5 shows an enlargement of the groove and ridge motif on the surfaces of the (0$\bar{1}$1) face of L-Leu-L-Leu-L-Tyr and the (01$\bar{1}$) face of D-Leu-D-Leu-D-Tyr. The face is viewed edge on, with the in-plane direction being perpendicular to the groove. The ridge and groove walls are delimited by uninterrupted stacking of the side chains. Particularly evident in the figures are the leucines (left-hand side of the groove), indicated by "leu", and tyrosines (right-hand side of the groove), indicated by "tyr". The difference between the two enantiomeric crystal faces is expressed in the orientation of the peptide stacking relative to the geometrical features (ridges and grooves) of the surfaces. Note however that the surface exposed to the antibody is the unmasked one only. In other words, the antibody detects a repetitive pattern of side chains spaced 5 Å apart in the direction of the *a* axis, with very little topographic relief; the side chains are all identical. The topography is very pronounced in the shape of the groove and ridge motif, but not when sliding along the surface of the groove itself at a higher resolution, which is needed to distinguish between the enantiomorphous structures. The recognition shown by antibody 48E is thus not trivial, and indicates a very high resolution of sterical interactions.

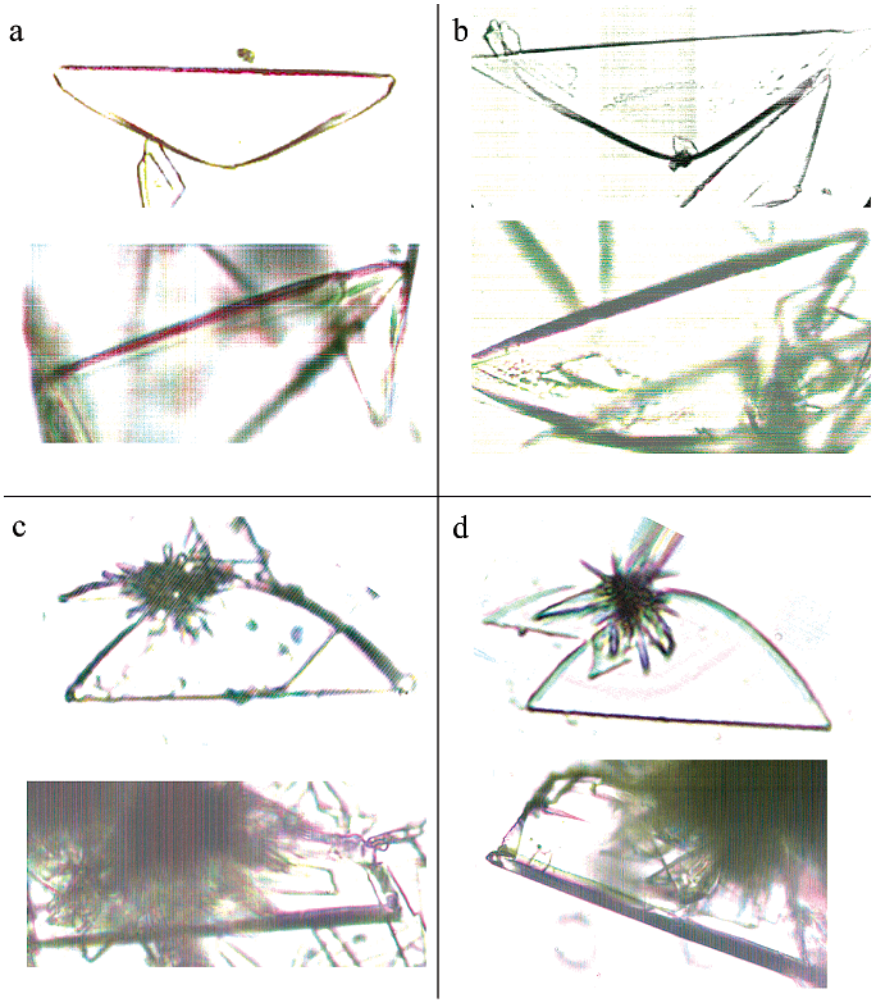

Figure 3. Crystals of Leu-Leu-Tyr incubated with antibody 48E and developed with the Vector-Red kit: red color is developed where antibody is adsorbed. (a) Crystals of L-Leu-L-Leu-L-Tyr incubated with antibody 48E. Only the $(0\bar{1}1)$ face is red. (b) Control crystals of L-Leu-L-Leu-L-Tyr in the absence of antibody. None of the crystal faces are colored red. The dominant blue-green color, especially evident in crystal aggregates, results from interaction of "white light" with the crystal and with the optical setup of the light microscope. (c) Crystals of D-Leu-D-Leu-D-Tyr incubated with antibody 48E. None of the crystal faces are colored red. (d) Control crystals of D-Leu-D-Leu-D-Tyr treated as in (b). None of the crystal faces are colored red.

It is no surprise, given the above, that the (001) face is not recognized by either antibody, as both its chemical nature and topography are different (Figure 1).

Discussion

Crystals of L-Leu-L-Leu-L-Tyr have been used to elicit and select specific monoclonal antibodies after immunization of a mouse with the crystals. The interactions of two of these antibodies with crystals of L-Leu-L-Leu-L-Tyr and D-Leu-D-Leu-D-Tyr were compared and contrasted. Antibody 48E binds only to one face of the L-Leu-L-Leu-L-Tyr crystals, but not to the same face of D-Leu-D-Leu-D-Tyr crystals. In contrast, antibody 602E binds crystals of L-Leu-L-Leu-L-Tyr at a family of related surfaces and shows no chiral discrimination between the L-Leu-L-Leu-L-Tyr and the D-Leu-D-Leu-D-Tyr crystals.

The face specificity exhibited by antibody 48E must be due to prominent differences in the structural complementarity between the antibody and the different crystal faces. The fact that the antibody can discriminate between the enantiomeric surfaces, despite their topographic similarity (Figure 5), is an impressive demonstration of the recognition power of the immune system.

The antibody variable regions were sequenced, and highly reliable structural models of their binding sites were derived, following a procedure similar to that developed and reported previously.[15,31−33] The complete description and analysis of the models and of their docking to the crystal surfaces will be the subject of a separate communication (M. Geva, L. Addadi, and M. Eisenstein, manuscript in preparation). The models show that the binding site of antibody 48E fits into the highly structured grooves at the surface of the $\{0\bar{1}1\}$ crystal faces with remarkable structural complementarity (Figure 6). The contact area between the antibody and the crystal face is very large. The chemical complementarity over the whole area is also very good, resulting in extensive hydrogen-bonding and hydrophobic interactions. The accumulation of these interactions yields high binding enthalpy and thus strong binding of the antibody to the crystal face. Docking of this antibody to the other surfaces resulted in fits that are not nearly as good as on the selected face. Only a few chemical interactions are consequently possible.

(31) Katchalski-Katzir, E.; Shariv, I.; Eisenstein, M.; Friesem, A. A.; Aflalo, C.; Vakser, I. A. *Proc. Natl. Acad. Sci. U.S.A.* **1992**, *89*, 2195−2199.
(32) Eisenstein, M.; Shariv, I.; Koren, G.; Friesem, A. A.; Katchalski-Katzir, E. *J. Mol. Biol.* **1997**, *266*, 135−143.
(33) Eisenstein, M.; Katchalski-Katzir, E. *Lett. Pept. Sci.* **1998**, *5*, 365−369.

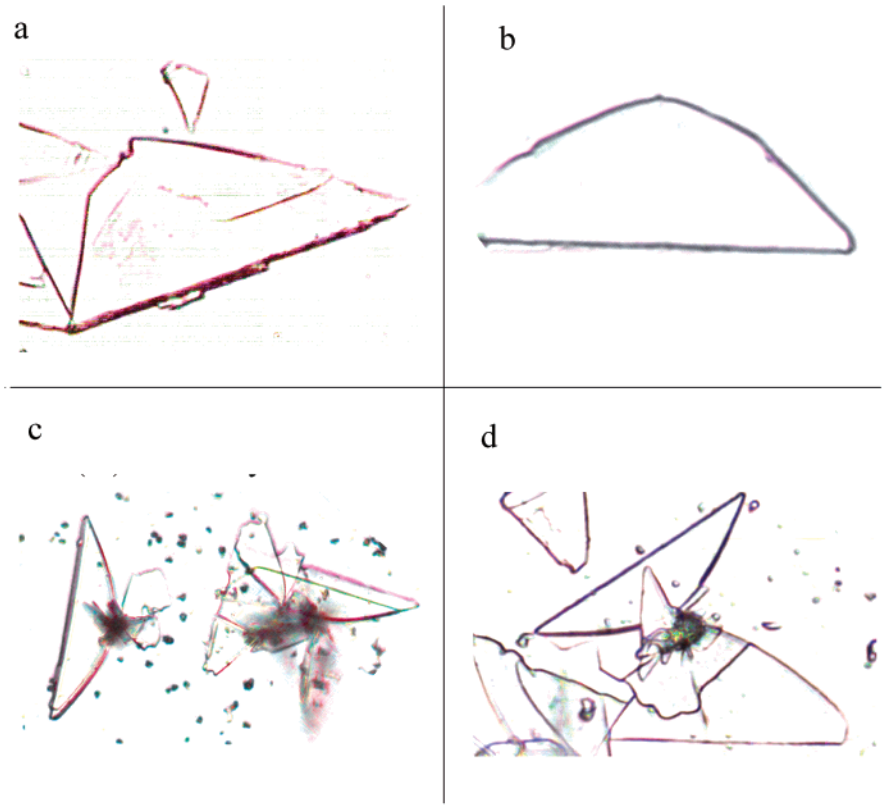

Figure 4. Crystals of Leu-Leu-Tyr incubated with antibody 602E and developed with the Vector-Red kit: red color is developed where antibody is adsorbed. (a) Crystals of L-Leu-L-Leu-L-Tyr incubated with antibody 602E. All peripheral faces are colored red. (b) Control crystals of L-Leu-L-Leu-L-Tyr in the absence of antibody. None of the crystal faces are colored red. The dominant blue-green color results from interaction of white light with the crystal and with the optical setup of the light microscope. (c) Crystals of D-Leu-D-Leu-D-Tyr incubated with antibody 602E. All peripheral faces are colored red. (d) Control crystals of D-Leu-D-Leu-D-Tyr treated as in (b). None of the crystal faces are colored red.

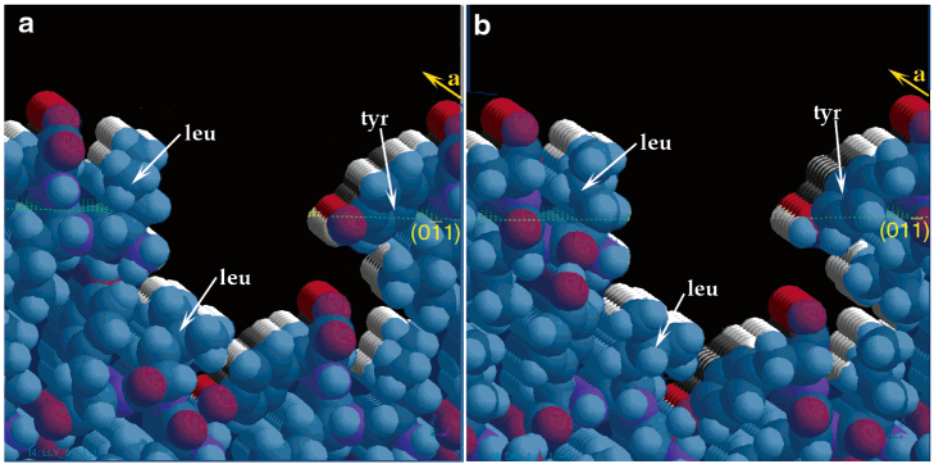

Figure 5. Close-up of the surface topography on the (0$\bar{1}$1) face of L-Leu-L-Leu-L-Tyr crystals (a) and on the (01$\bar{1}$) face of D-Leu-D-Leu-D-Tyr crystals (b). The groove and ridge motif is almost edge-on to the plane of view. The antibody accesses the surface from above. A semitransparent blue mask has been introduced to mask the atoms that are not accessible from the surface. The dashed yellow lines mark the plane directions. The solid yellow arrows indicate the direction of the *a* axis, parallel to the groove. The *b* and *c* axes are in plane, oblique to the surface. The color code is as in Figure 1.

The enantioselectivity of antibody 48E, on the other hand, is not evident in the docking models. Nevertheless, an extremely good fit of the antibody to the crystal and numerous hydrogen bond interactions and aromatic−aromatic interactions are evident in the docking model. These interactions are geometrically constrained, and may thus account for chiral discrimination. The fact that antibody 48E can effectively distinguish between the two surfaces indicates the astounding high resolution of the antibody's recognition. To our knowledge, such a high level of structural complementarity between proteins and crystal surfaces has been demonstrated only in antifreeze proteins vis-à-vis specific crystal faces of ice,[34,35] besides the antibodies selected against crystal surfaces.[15,21,28]

In contrast to 48E, the models show that binding of antibody 602E to the {0$\bar{1}$1} and {*hk*0} faces on both the L-Leu-L-Leu-

(34) Liou, Y. C.; Tocilj, A.; Davies, P. L.; Jia, Z. C. *Nature* **2000**, *406*, 322−324.

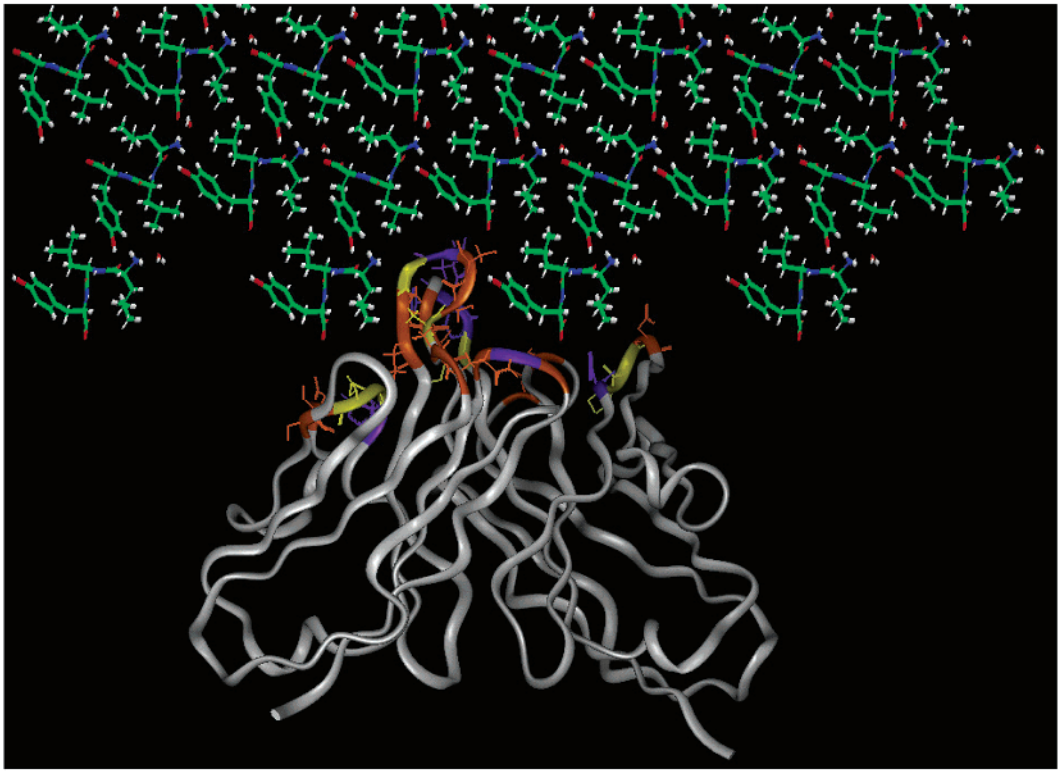

Figure 6. Model of the variable region of antibody 48E (in ribbon representation) docked on the surface of the $(0\bar{1}1)$ face of the L-Leu-L-Leu-L-Tyr crystal (in stick representation; C, green; H, white; N, blue; O, red). Only the side chains on the loops of the antibody binding site are represented and colored. Color code for the antibody: yellow, hydrophobic residues; purple, aromatic residues; orange, hydrophilic residues. Note that the yellow sections are juxtaposed to the leucine side chains of the tripeptide crystal, the purple sections are juxtaposed to the crystal tyrosine aromatic rings, and the orange sections are juxtaposed to the crystal carboxylate termini and to its tyrosine hydroxyls.

L-Tyr and the D-Leu-D-Leu-D-Tyr crystals is driven by electrostatic interactions. The binding site of antibody 602E exposes four charged residues, while antibody 48E does not expose any charged residues. We surmise that the presence of charged residues at the binding site enables binding of the antibody to different surfaces, even if the topographical complementarity between the surfaces is less than optimal and there is relatively low contact area. The enthalpic contribution of the electrostatic interactions is overwhelming and compensates for the low contribution of other interactions. A similar case was reported previously[15] for antibodies 36A1 and 23C1, which were raised and selected against crystals of cholesterol and 1,3-dinitrobenzene, respectively. Antibody 36A1 was shown to preferentially bind to one specific crystal face, while antibody 23C1 is a cross-reactive antibody, binding to high-energy sites on crystal surfaces. The amino acid sequences of the variable regions of the two antibodies have 91% identity. However, antibody 23C1 has three charged residues exposed at its binding site, whereas the binding site of antibody 36A1 has none.

A range of levels of resolution in surface recognition has been encountered in the two systems studied so far, namely, cholesterol[23] and the tripeptides studied here. Antibody 23C1[15] binds to various crystals, is not stereospecific, and is obviously not enantiospecific. Antibody 602E has low stereospecificity and no enantiospecificity. Antibody 36A1[15] has extremely high stereospecificity, but no enantiospecificity.[23] Finally, antibody 48E is stereospecific and enantiospecific. These few examples highlight how chiral recognition at surfaces is intrinsically different from chiral recognition between biological macromolecules and single molecular epitopes. In the latter case, the molecular asymmetry is fully expressed at the interface, and chiral recognition depends on the nature, extent, and complementarity of the interactions established between the epitope and the antibody binding site. Chiral recognition between antibodies and enantiomeric surfaces depends, in addition to the above, on an additional level, namely, the extent of dissimmetry expressed at the crystal surface.

The use of crystals as antigens has provided a depth of structural insight into antibody−surface interactions that is normally not available in biology. This can potentially be applied to biological systems, to derive structural information that is difficult to achieve otherwise. One application is the understanding of the evolution of macroscopic chirality in biology. A more practical application is the elucidation of the molecular organization of biological surfaces. The presence of organized cholesterol-rich microdomains in cell membranes is now well established.[36] The so-called "cholesterol rafts" appear to be crucial in cell trafficking and signaling,[37] as well as in the development of various diseases.[38,39] Very little information is however available on their structural organization. Probing the surfaces with a battery of well-characterized, structure-sensitive antibodies might provide some of this information. In a recent

(35) Graether, S. P.; Kuiper, M. J.; Gagne, S. M.; Walker, V. K.; Jia, Z. C.; Sykes, B. D.; Davies, P. L. *Nature* **2000**, *406*, 325−328.

(36) Simons, K.; Ikonen, E. *Nature* **1997**, *387*, 569−572.
(37) Simons, K.; Toomre, D. *Nat. Rev. Mol. Cell Biol.* **2000**, *1*, 31−39.
(38) Chochina, S. V.; Avdulov, N. A.; Igbavboa, U.; Cleary, J. P.; O'Hare, E. O.; Wood, W. G. *J. Lipid Res.* **2001**, *42*, 1292−1297.

demonstration of this concept, one antibody selected on cholesterol monohydrate crystals was used to label cholesterol microdomains in macrophages and fibroblasts whose membranes were enriched with cholesterol.[40]

Acknowledgment. We are grateful to Orit Leitner, Anat Bromberg, and Alon Levy for their help in monoclonal antibody production, to Genevieve Vicenti-Brown for performing some crystallization experiments, and to David Michaeli and Aurelie Lachish-Zalait for some of the syntheses. L.A. is incumbent of the Dorothy and Patrick Gorman Professorial Chair, and M.G. is the recipient of the Jeaninne Klueger Scholarship. This work was supported by a grant from the Israel Science Foundation, administered by the Israel Academy of Sciences.

JA027942J

(39) Ono, A.; Freed, E. O. *Proc. Natl. Acad. Sci. U.S.A.* **2001**, *98*, 13925−13930.
(40) Kruth, H. S.; Ifrim, I.; Chang, J.; Addadi, L.; Perl-Treves, D.; Zhang, W. Y. *J. Lipid Res.* **2001**, *42*, 1492−1500.